The Effect of Tin Addition to ZnO Nanosheet Thin Films for Ethanol and Isopropyl Alcohol Sensor Applications

Brian Yuliarto[1,2*], Sri Julia[1], Ni Luh Wulan S.[1], Muhammad Iqbal[1], Muhammad F. Ramadhani[1] & Nugraha[1]

[1]Materials Processing Laboratory, Engineering Physics Research Group,
Institut Teknologi Bandung, Jalan Ganesha No. 10, Bandung 40132, Indonesia
[2]National Research Center for Nanotechnology (NRCN),
Institut Teknologi Bandung, Jalan Ganesha No. 10, Bandung 40132, Indonesia
Email: brian@tf.itb.ac.id

Abstract. The requirements of green environmental and public health monitoring have become stricter along with greater world attention for global warming. The most common pollutants in the environment that need tightened control are volatile organic compounds (VOC). Compared to other kinds of sensors, semiconductor sensors have certain advantages, including high sensitivity, fast response, simplicity, high reliability and low cost. In this work, ZnO and Sn-doped ZnO nanostructure materials with high surface nanosheet areas were synthesized using chemical bath deposition. The X-ray diffraction patterns could be indexed according to crystallinity mainly to a hexagonal wurzite ZnO structure. The scanning electron microscopy (SEM) results showed that in all samples, the thin films after the addition of Sn consisted of many kinds of microstructure patterns on a nanoscale, with various sheet shapes. The sensor performance characterizations showed that VOC levels as low as 3 vol% of isopropyl alcohol (IPA) and ethanol could be detected at sensitivities of 83.86% and 85.57%, respectively. The highest sensitivity of all sensors was found at an Sn doping of 1.4 at%. This high sensor sensitivity is a result of the high surface area and Sn doping, which in turn produced a higher absorption of the targeted gas.

Keywords: *chemical bath deposition ethanol; gas sensor; isopropyl alcohol; nanosheets; thin films; tin; zinc oxide.*

1 Introductions

The requirements of green environmental and public health monitoring have become stricter along with greater world attention for green development and global warming. Among the most common hazardous pollutants in the environment that need to be controlled intensively are volatile organic compounds (VOCs). The main sources of outdoor VOCs are combustion processes, motor vehicles and fuel evaporation. However, as many people spend most of their daily time indoors, such as in offices, homes, or shopping malls, the health of indoor environments should also receive attention. In fact, the

Received June 1st, 2014, Revised December 13th, 2014, Accepted for publication December 29th, 2014.
 ISSN: 2337-5779, DOI: 10.5614/j.eng.technol.sci.2015.47.1.6

indoor concentrations of VOCs are 2-5 times higher than their corresponding outdoor concentrations. The poor quality of indoor air has been linked to a number of symptoms, which the World Health Organization defines as the sick building syndrome [1]. These symptoms include headaches, nausea, irritation of the eyes, mucous membranes in the respiratory system, drowsiness, fatigue and general malaise. Poor air quality in office premises produces discomfort, decreases worker efficiency and increases absenteeism. Conversely, improved air quality can lead to improved productivity [2].

The primary instrument for environmental monitoring is a gas monitoring system consisting of a gas-sensitive layer that acts as a sensor. Compared to other kinds of sensors, semiconductor sensors have advantages such as high sensitivity, fast response, simple, high reliability, and low cost [3]. Two types of semiconductor materials that are widely used for this purpose are zinc oxide and stannic oxide [4]. Researchers have used ZnO in different forms, such as thick films, thin films, nanowires, nanoparticles and nanorods, depending on the application [5-8]. Many researchers are attracted to develop ZnO for monitoring systems due to its low cost, its mature synthesis technology, its tunable properties and large exiton binding (60 eV). ZnO is an n-type direct wide band gap semiconductor (E_g = 3.35 eV at near room temperature) that has excellent chemical and thermal stability with optoelectronic properties and a strong piezoelectric effect [9-11]. Extensive efforts have been focused on improving sensor performance in detecting targeted gases in terms of properties such as sensitivity, selectivity and time response.

In the development of gas sensors several methods to improve performance have been tested. One technique is to increase the interactive surface layer of the sensor material by constructing nanostructure metal oxide resulting in enhanced sensitivity through more depletion of the absorbed carrier trapped on the surface states within the nanostructure. Efforts have been directed at fabricating one-dimensional (1D) nanostructures, such as nanowires, nanotubes or nanosheets, because of their unique physical and chemical properties [9-15]. An alternative technique for improving sensor response is to prepare the sensor material with various doping materials [16,17]. The dopants of ZnO can be from either noble materials or metal oxide due to the formation of p-n junctions or the catalytic activity of those materials.

However, so far, research that combines the above approaches still needs to be explored further [18], especially for VOC gas sensors. In this work, ZnO nanostructure materials with high surface area nanosheet patterns with Sn-dopant have been synthesized using chemical bath deposition. The resulting ZnO nanostructure thin films were characterized with x-ray diffraction and scanning electron microscopy in order to investigate the surface structure. Sn-

doped ZnO nanosheet thin films that may possess a nanostructure and dopant effects have been systematically examined for application as sensors of ethanol and isopropyl alcohol.

2 Experiments

Depositions of thin film as a sensitive layer were prepared through a wet chemical method known as chemical bath deposition. First, alumina (Al_2O_3) – used in this study as the substrate – was rinsed with deionized water and ethanol using ultrasonic bath cleanser for 10 minutes, respectively. The substrate was 12.5 mm x 12.5 mm in dimension and had a pair of silver interdigitated electrodes printed on top of it. In order to prepare the precursor solution, zinc nitrate tetrahydrate, $Zn(NO_3)_2 \cdot 4H_2O$ (Merck) 0.15 M, was used as the precursor; $SnCl_2 \cdot 4H_2O$ (Merck) as the dopant precursor; urea (Merck) as the catalyst and ethanol mixed with deionized water as the solvent. The precursors and catalyst were stirred in the solvent for 1 hour to obtain a homogenous solution. The substrate was then immersed in the solution at 60°C for 48 hours. Crystal growth on the substrate was actuated through aging. Moreover, in order to increase the crystallinity of the ZnO and the Sn-doped ZnO, the resulting thin film samples were calcined at 300°C for 30 minutes.

To characterize the after-synthesized thin films an X-ray diffractometer (XRD) was used in order to investigate the crystal phase. A scanning electron microscope (SEM) was employed to study the morphological surface of the thin films. The XRD analysis was obtained using a Philips 1835 diffractometer scanning the region of $2Ø$ = 10-90° with Cu Kα radiation. Scanning electron microscopy was carried out with a Jeol JSM-6510LV (Japan) low vacuum scanning electron microscope. Furthermore, to investigate the sensing performance of the sample toward the target gases (VOCs), the samples were tested with a sensing performance measurement system, configured as shown in Figure 1. The sample was placed into a gas sensor test chamber and heated up to certain temperatures that were controlled with an Omron E5CK digital temperature controller and a G3PX-220EH power controller. In this study, the operating temperature was varied at 200°C, 250°C, and 300°C. Before the sample was exposed to the target gases – ethanol and isopropyl alcohol (IPA) – ambient air was introduced into the test chamber for 30 minutes in order to check the baseline resistance of the sample. The electrical resistance response of the sample was acquired with a Picotest M3500A digital multimeter and recorded by computer. Nitrogen gas was used to control the concentrations as well as the gas carrier in order to evaporate the VOCs in the bubbler and flow them through a pipe into the test chamber where the sample was placed. When the nitrogen and the target gases (ethanol and isopropyl alcohol) were flown through the test chamber, the corresponding steady state resistance of the sensor

in ambient air (R_a) and in the presence of the target gas (R_g) was measured. The response sensitivity of a sensor to reducing gases (such as ethanol and IPA) is defined as,

$$S = \left(\frac{R_a - R_g}{R_g}\right) \times 100\% \quad (1)$$

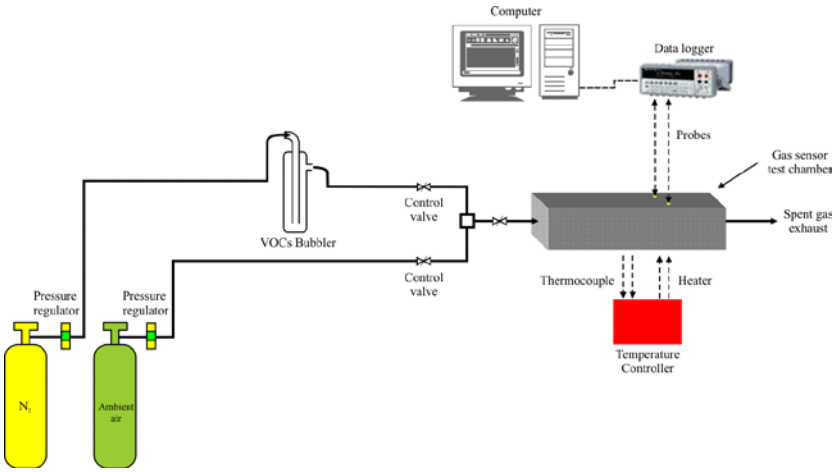

Figure 1 The testing diagram for VOC sensor characterization.

3 Results and Analysis

The crystal structure of both the pure ZnO nanostructure sample and the Sn modified ZnO nanostructure samples was characterized by X-ray diffraction (XRD). Figure 2(a) shows the XRD measurement results of the pure ZnO nanostructure grown on alumina substrate. Figure 2(b), (c) and (d) are the XRD results of the Sn-modified ZnO nanostructure in various Sn-doping concentrations. All the diffraction peaks could be indexed according to crystallinity mainly to hexagonal wurzite ZnO (referring to JCPDS No. 36-1451). Moreover, the XRD patterns showed that there was no significant change after the addition of the Sn, indicating that the crystallization of the formed thin film was successful. The dashed lines in Figure 2 show that in all XRD diffraction patterns of the various Sn-doping amounts, the crystallinity peaks occurred at exactly the same position of the 2Ø range. There was no shift in the 2Ø angle of the XRD patterns, which indicates that after the addition of all varying amounts of Sn, the ZnO thin film structures had not been changed.

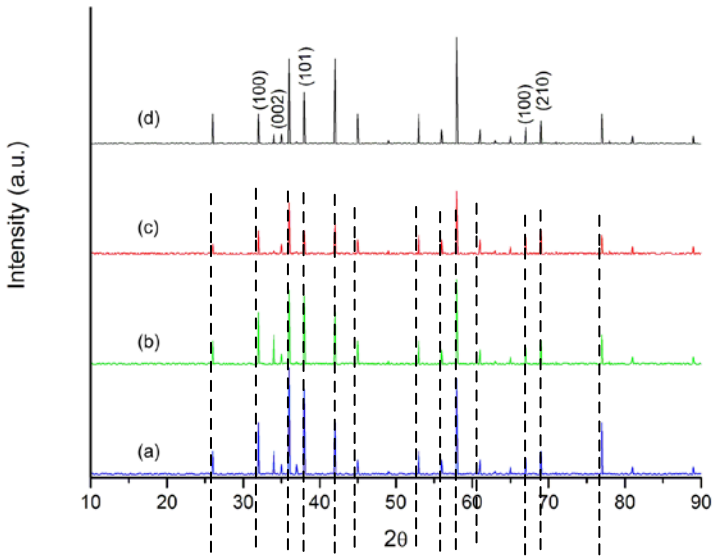

Figure 2 Diffraction pattern of (a) pure ZnO, (b) 1.2 at% Sn-doped ZnO, (c) 1.4 at% Sn-doped ZnO, and (d) 1.5 at% Sn-doped ZnO.

The microstructure morphology of the samples was analyzed by scanning electron microscopy, as shown in Figure 3. It can clearly be seen that all the samples after the addition of Sn consisted of many kinds of microstructure patterns on a nanoscale, with different shapes. Moreover, it can also be observed that the surface morphology of the thin films was strongly dependent on the amount of Sn as dopant. The amount of nanosheet structures increased as the Sn was added up to 1.4 at%. Figure 3(a) shows that the sheets were not uniform and the structures only appeared in small amounts. After addition of 1.2 at% of Sn, the small sheets had grown and yielded a more uniform structure, as shown in Figure 3(b). After the addition of Sn reached 1.4 at%, the sheet structure became more uniform, as shown in Figure 3(c). As the Sn was continued to be increased to over 1.4 at %, the merged sheet structure produced smaller nanosheets in the films, as shown in Figure 3(d). This phenomenon would has a positive relationship with the surface area, where a more uniform nanostructure correlates with a higher surface area. Therefore, the addition of 1.2 at% of Sn and 1.4 at% of Sn increased the surface area as the nanostructure grew and became more uniform. Moreover, the merged nanostructure and smaller nanosheets resulted in a decreasing surface area as the addition reached 1.5 at% of Sn.

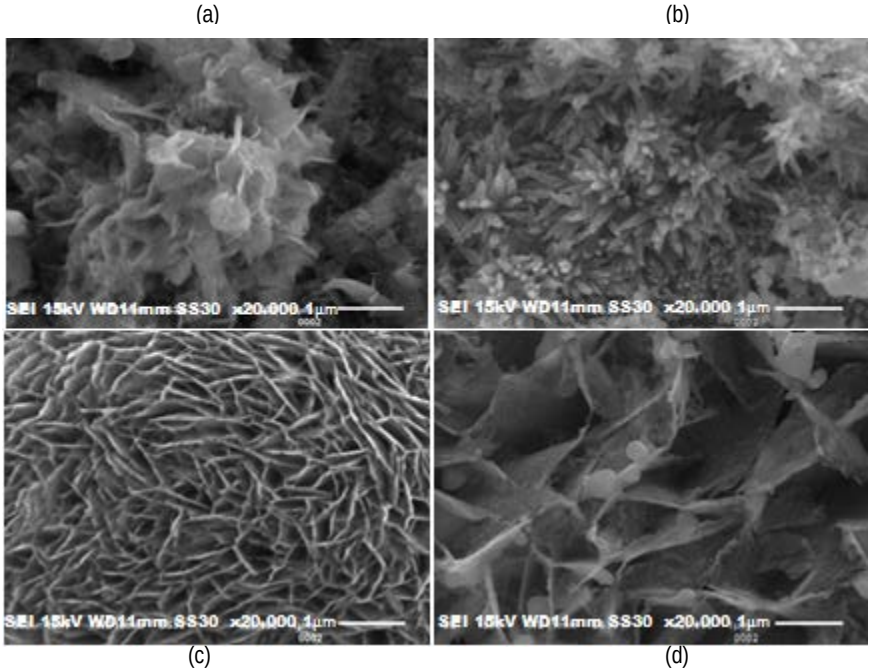

Figure 3 Morphological surface of the synthesized samples from SEM measurement: (a) pure ZnO, (b) 1.2 at% Sn-doped ZnO, (c) 1.4 at% Sn-doped ZnO, and (d) 1.5 at% Sn-doped ZnO.

The resulting sensor devices with various concentrations of Sn-doping were investigated further to study their sensing characteristics for ethanol and isopropyl alcohol gas. Figure 4 shows the typical measurements of the sensor's dynamic response to characterize their sensitivity. Before exposing the samples to ethanol vapor, ambient air was introduced into the testing chamber for one hour to determine the initial stable electrical resistance in order to ensure a stable zero level for gas sensing applications. N2 gas was flowed through the ethanol bubbler in order to evaporate the ethanol in the testing room where the thin-film sensor device was placed. When the N2 and ppm-level target gases were streamed through the test chamber, the corresponding steady state resistances of the sensor in ambient gas (Ra) and in the presence of the target gas (Rg) were recorded. The sensor response to decreasing gas amounts (in this case, ethanol and isopropyl alcohol) is defined in Eq. (1). Figure 4 clearly shows that an increase in gas concentration increased the sensor response, which also increases the sensor's sensitivity. The sudden exposure to the targeted gases quickly changed the resistivity of the devices, which indicates that the sensors have a fast response time as well as recovery time.

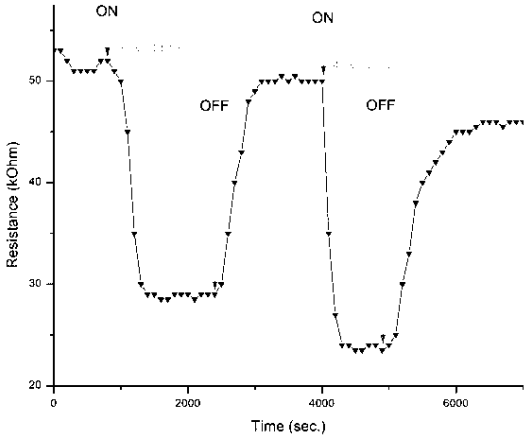

Figure 4 Dynamic response of the sample 1.2 at% Sn-doped ZnO exposed by 3 vol% and 4 vol% EtOH at 200°C.

The ethanol vapor sensing mechanism of the sample can be explained as follows. The adsorption of atmospheric oxygen on the sample surface forms ionic species such as O_2^- and O^- which acquire electrons from the conduction band. The kinetic reactions before and after ethanol exposure that probably occur are described in Eq. (2), (3), (4), and (5) [19-22].

$$O_2\,(gas) \leftrightarrow O_2\,(ads) \tag{2}$$

$$O_2\,(ads) + e^- \leftrightarrow O_2^-\,(ads) \tag{3}$$

$$O_2^-\,(ads) + e^- \leftrightarrow 2O^-\,(ads) \tag{4}$$

As gas exposure on the sample decreases (in this case ethanol and isopropyl alcohol vapor), the vapor particles react with the oxygen ions. These reactions break the oxygen and electron bonds, thus leading the electrons to return to the conduction band, which will decrease the resistance of the sample:

$$C_nH_{2n+1}OH + O^- \rightarrow C_nH_{n+1}OH + H_2O + e^- \tag{5}$$

The explanations from Eq. (1) to Eq. (5) imply that the sensing performance depends on the interaction between the targeted gases and the surface of the sensitive layer. Figure 5 shows the sensing mechanism process, where the targeted gas and the oxygen in the air only interact with the sensitive layer of the Sn-modified ZnO nanostructure. As a result there are no effects from the thickness of the thin films. The sensitive surface layers would play a dominant role in this process. Consequently, the surface area, which is influenced by the nanostructure of the Sn-ZnO thin films, would be an important factor in terms of improving sensing performance.

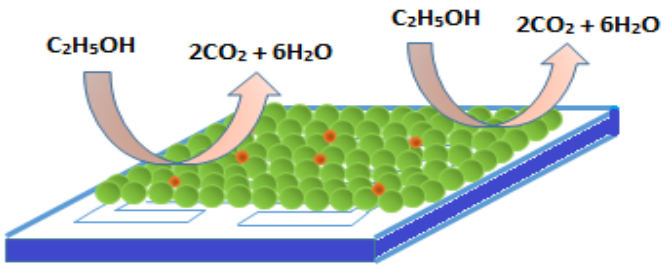

Figure 5 Illustration of the interaction between the targeted VOC gases and the sensor occurring only at the surface of the sensitive layer of the Sn-modified ZnO thin films.

Figure 6 shows the dynamic response of the sensor to different concentrations of ethanol with variation of the operating temperature at 200°C, 250°C and 300°C, respectively. The ethanol gas was varied between 3 vol% and 4 vol%. These measurements were meant to identify the optimum operating temperature of the sensor devices for ethanol exposure. When the sensors' responses are compared between low and high concentrations of ethanol, it can clearly be seen that higher concentrations of ethanol yield a higher shift of the sensor response. This phenomenon occurs in all temperature cases, which indicates that the sensor has good linearity as a function of operating temperature for ethanol gas. Plots of sensitivity as a function of operating temperature are shown in Figures 6 and 7. It can clearly be seen in Figure 6 that the concentration of 1.4 at% Sn-dopant yielded the best sensing response of all concentrations, regardless of the operating temperature.

Figure 7 shows the sensor's dynamic response to different isopropyl alcohol concentrations with operating temperatures varied at 200°C, 250°C and 300°C, respectively. These measurements were meant to determine the optimum device operating temperature for each sensor after exposure to isopropyl alcohol gas. When the sensors' responses to low and high isopropyl alcohol concentrations are compared, it can clearly be seen that the higher isopropyl alcohol concentrations produced a higher shift in the sensor's response. This occurred for all operating temperatures, indicating that the sensor has good linearity in terms of operating temperature for isopropyl alcohol gas.

The sensor sensitivity responses for ethanol gas and IPA gas are shown in Tables 1 and 2, respectively. The highest sensitivity was observed at an operating temperature of 250°C for all doping concentrations. From the sensitivity responses both for IPA and ethanol as shown in the Table 1 and Table 2 it can clearly be seen that the sensors had almost the same response to the IPA and the ethanol. The sensitivity values of the sensors had almost the

same value for any variation of working temperature or targeted vapor concentration. This phenomenon indicates that the sensors may be expected to have the same response to others VOC gases.

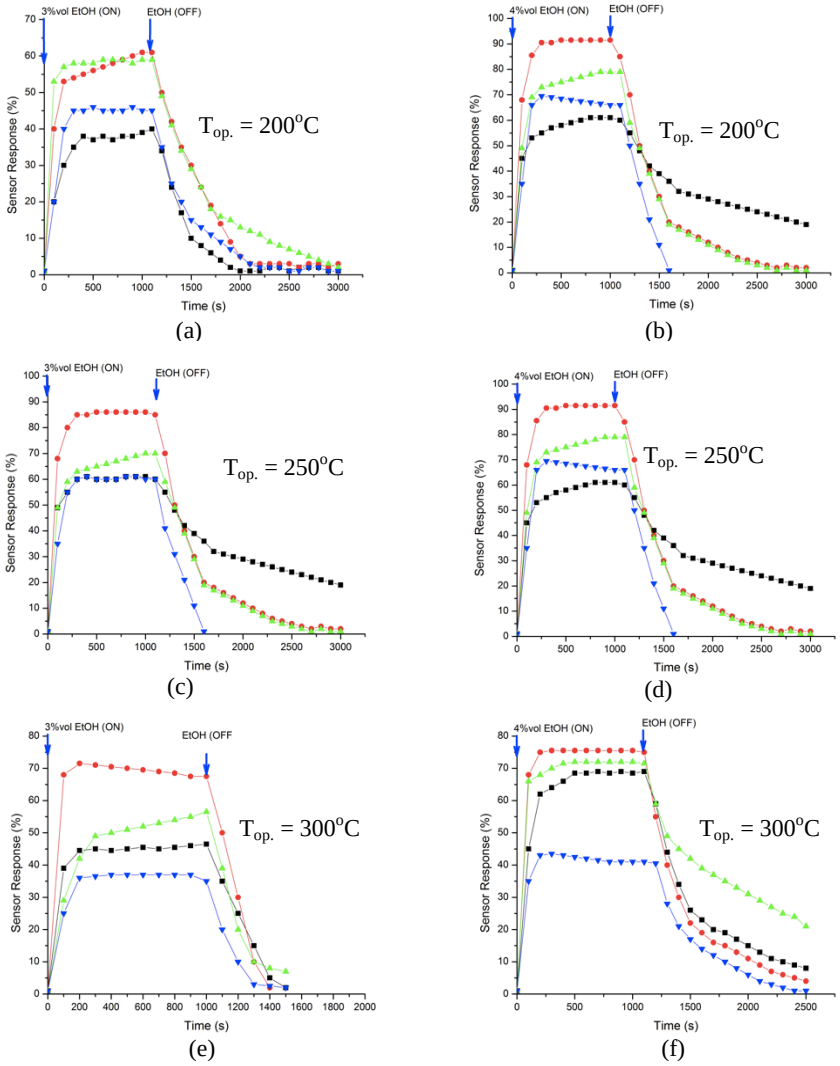

Figure 6 Dynamic characteristics of the sensors as a response to 3 vol% and 4 vol% of ethanol at (a) and (b) 200°C, (c) and (d) 250°C, (e) and (f) 300°C, respectively (for pure Zno, for 1.2% Sn-doped ZnO, for 1.4% Sn-doped ZnO, and for 1.5% Sn-doped ZnO).

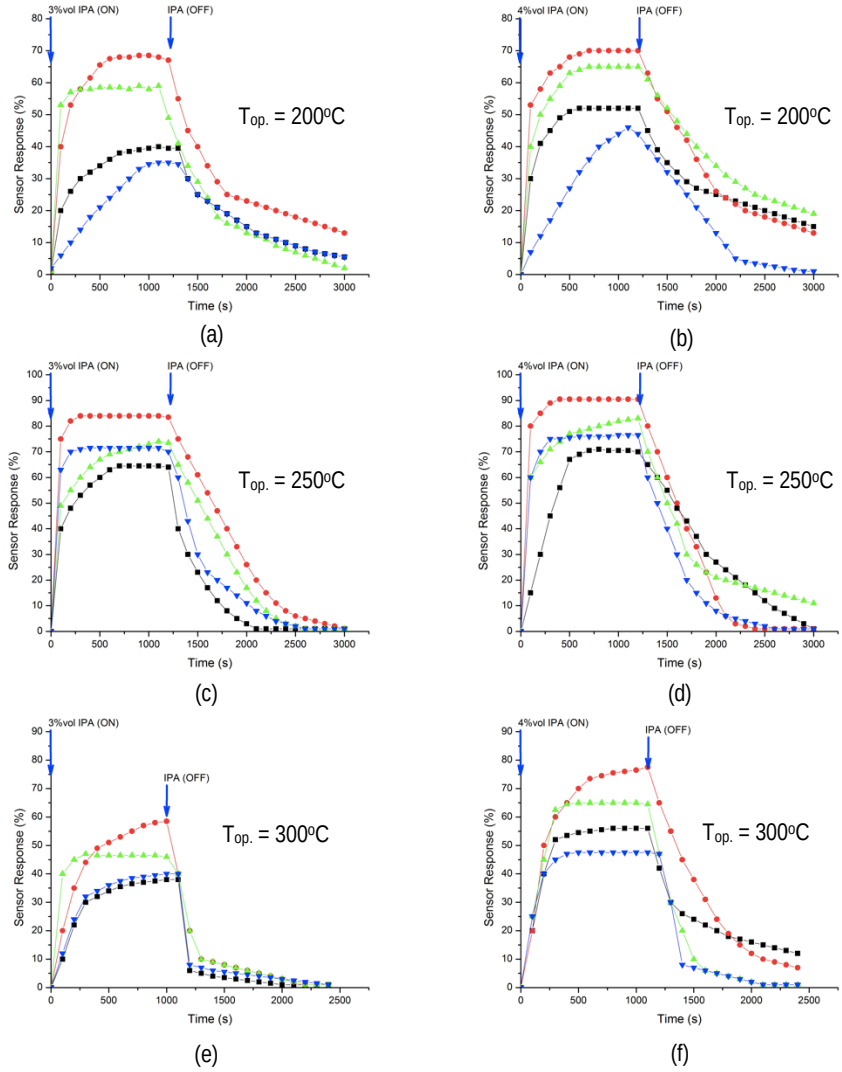

Figure 7 Dynamic characteristics of the sensors as a response to 3 vol% and 4 vol% isopropyl alcohol at (a) and (b) 200°C, (c) and (d) 250°C, (e) and (f) 300°C, respectively (for pure ZnO, for 1.2% Sn-doped ZnO, for 1.4% Sn-doped ZnO, and for 1.5% Sn-doped ZnO).

Sensor sensitivity as a function of operating temperature was plotted (Figure 8) in order to analyze the optimum sensor operating temperature. The sensor response depends on the removal of adsorbed O^-, O_2^-, O^{2-} and its ability to react with the ethanol vapor at a given temperature. The response and recovery times of the ZnO nanosheets to both ethanol and isopropyl alcohol gas at various

operating temperatures are shown in Figures 6 and 7. Since the permissible exposure limit (PEL) for ethanol according to OSHA (Occupational Safety & Health Administration, USA) is 12.75 vol% for 1 hour, this sensor seems to be a promising solution for ethanol and isopropyl alcohol detection based on the response and recovery time results [16].

Table 1 Responses of the sensor to 3 vol% and 4 vol% ethanol.

Temperature (°C)	Response (%)							
	3% vol				4% vol			
	0% Sn	1.2% Sn	1.4% Sn	1.5% Sn	0% Sn	1.2% Sn	1.4% Sn	1.5% Sn
200	33.00	78.02	69.05	38.03	45.01	65.08	70.02	50.00
250	62.44	70.08	85.57	63.54	75.05	80.09	90.04	67.02
300	38.01	47.00	59.05	36.06	45.07	63.07	78.02	52.01

Table 2 Responses of the sensor to 3 vol% and 4 vol% IPA.

Temperature (°C)	Response (%)							
	3% vol				4% vol			
	0% Sn	1.2% Sn	1.4% Sn	1.5% Sn	0% Sn	1.2% Sn	1.4% Sn	1.5% Sn
200	33.12	78.47	67.07	41.42	47.05	54.73	76.75	55.41
250	76.90	72.05	83.86	53.92	73.66	78.13	93.18	53.90
300	40.37	58.41	42.84	36.19	47.24	77.63	65.10	56.01

The increasing sensitivity has a positive correlation with the amount of Sn added into the ZnO from 1.2 at% to 1.4 at%. However, the sensitivity decreases when the amount of Sn continues to be added until 1.5 at%. These results have a positive correlation with the surface area analysis of the SEM results as described above. The addition of Sn until 1.4 at% yielded an increase of the surface area. Subsequently, the surface area decreased when the addition of Sn was continued up to 1.5 at%. Therefore, there is an optimum amount of Sn-doping that yields maximum sensitivity. Before exposure to ethanol and IPA, oxygen atoms are adsorbed into the ZnO surface, take electrons and become O^-. This ion sorption builds a depletion layer on the surface of the ZnO. The presence of ethanol or IPA decreases the depletion layer and reduces resistance. The ethanol or IPA takes the oxygen ions and releases electrons to the ZnO. Sn added into the ZnO will settle into the structure defects existing in the ZnO structure, which completes the ZnO structure. This complete structure allows the production of more oxygen that can be caught during reactions. Afterwards, an n-n junction will be built between them. Transfer of electrons occurring from Sn to ZnO creates an electron accumulation layer on the ZnO surface. This mechanism allows more oxygen to be adsorbed to the ZnO surface and enhances the response. However, when the Sn continues to be added into the ZnO beyond a certain point, the addition will produce new defects in the structure and produce less electrons on the surface, resulting in fewer oxygen

atoms that can be adsorbed into the surface. This turning point was observed in the case of 1.5 at% Sn-modified ZnO.

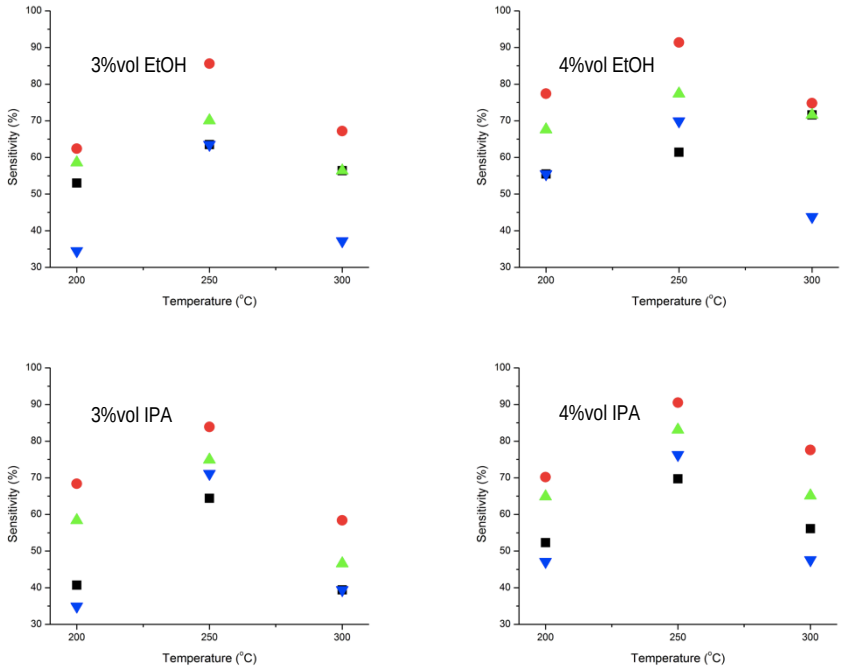

Figure 8 Sensitivity of pure ZnO and Sn-modified ZnO as a function of operation temperature (200°C, 250°C and 300°C) exposed by 3 vol% and 4 vol% EtOH (for pure ZnO, for 1.2% Sn-doped ZnO, for 1.4% Sn-doped ZnO and for 1.5% Sn-doped ZnO).

Figure 8 shows the sensitivity of the Sn-modified zinc oxide thin films after exposure to 3% and 4% of both ethanol and IPA vapor at various operating temperatures (200°C, 250°C and 300°C). The figure shows that at exposure to 3% ethanol vapor, the sensor's sensitivity increased as the temperature went up to 250°C and then decreased to 300°C. This phenomenon occured in all types of sensors, where the 1.4 at% sensor had the highest sensitivity compared to the other sensors. The sensitivity at 3 vol% of ethanol and IPA gas concentrations was 85.57% and 83.86%, respectively. Subsequently, for the ethanol concentration of 4 vol%, the sensitivity also increased as the temperature was increased to 250°C but it decreased at 300°C. This is possibly due to the fact that at a low temperature, a low response can be expected because the gas molecules do not have sufficient thermal energy to react with the surface-adsorbed oxygen species.

The relationship between working temperature and sensor conductivity can be seen in the Arrhenius plot in Figure 9. There is a dependence of the conductance on the temperature. The conductance increases as the temperature increases because at higher temperatures more electrons in the valence band have sufficient energy to jump to the conduction band. As a result, the sensor conductance will increase. The conductance will also increase when the samples are exposed to 3 vol% of IPA vapor. IPA presence on the sensor surface will decrease the activation energy from 4.99 eV to 3.35 eV. The smaller activation energy means it will be easier for electrons to jump to the conduction band. The sensor's response increases from 200°C to 250°C and then decreases at 300°C. At 250°C, the physical adsorption and chemical reaction reach optimal condition. When the temperature is higher than 250°C, the physical adsorption will decrease, because the rate of desorption increases, resulting in a decreased sensitivity.

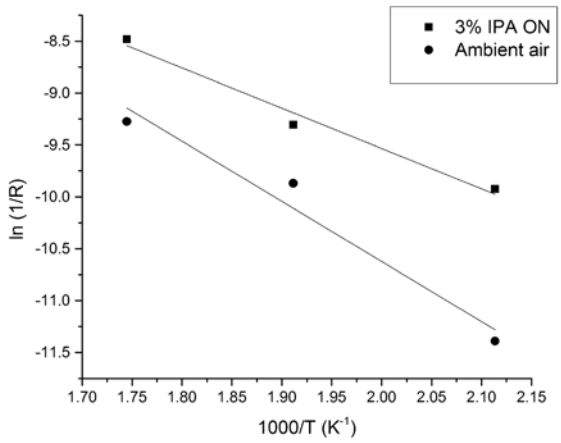

Figure 9 Arrhenius plot of the Sn-modified ZnO nanostructure thin films on ambient air and the targeted gas (3% IPA).

In the reaction between the sensor and the targeted gas, there are two possibilities, explained as follows: at low temperatures, the sensor response is restricted by the speed of the chemical reaction, while at higher temperatures it is restricted by the speed of the diffusion of the gas molecules. At a certain intermediate temperature, the speed values of both processes becomes equal, at which point the sensor response reaches its maximum. Thus, in the present case, the optimum operating temperature for the Sn-modified ZnO nanostructure films was 250°C, at which the sensor response attained its peak value. The best sensitivity of the sensors for both ethanol and isopropyl alcohol gas was clearly observed at an operating temperature of 250°C.

4 Conclusions

Nanostructured ZnO and Sn-doped ZnO thin films were successfully synthesized through a simple chemical bath deposition method. XRD characterization showed that the synthesized material had a wurtzite phase and the micrograph obtained from a scanning electron microscope showed that the materials had nanostructured grains distributed well in the films. The sensing characteristics of the materials toward various percentage levels of VOC vapors were investigated at various operating temperatures. The materials exhibited a good performance in detecting the presence of ethanol as well as isopropyl alcohol. Addition of Sn-dopant further increased the sensitivity of the sensor response until an optimum dopant addition amount of 1.4 at%. It has been established that the sensing response of metal oxide based semiconductor gas sensors has an optimum operating temperature, identified in this study at 250°C. Finally, the highest sensitivity of 1.4 at% Sn-doped ZnO was 91% with a response time of 70 seconds.

Acknowledgements

This work was partially supported by Penprinas MP3EI, Ministry of Education and Culture, 2013 and SINas Research Incentive Program, Ministry of Research and Technology **(RT-2013-731)**, Republic of Indonesia, who are gratefully acknowledged.

References

[1] Kostiainen, R., *Volatile Organic Compounds in the Indoor Air of Normal and Sick Houses,* Atmospheric Environment, **29**(6), pp. 693-702, 1995.

[2] Fernandes, M.B., Brickus, L.S.R., Moreira, J.C. & Cardoso, J.N., *Atmospheric BTX and Polyaromatic Hydrocarbons in Rio de Janeiro, Brazil,* Chemosphere, **47**(4), pp. 417-25, 2002.

[3] Sadek, A.Z., Choopun, S., Wlodarski, W., Ippolito, S.J. & Kalantar-Zadeh, K., *Characterization of ZnO Nanobelt-based Gas Sensor for H_2, NO_2, and Hydrocarbon Sensing*, IEEE Sensors Journal, **7**, pp. 919-924, 2007.

[4] Mishra, R.K., Upadhyay, S.B. & Sahay. P.P., *Volatile Organic Compounds (VOCs) Response Characteristics of the Hydrothermally Synthesized SnO_2 Nanocapsules*, Sensor Lett., **11**, pp. 1611-1616, 2013.

[5] Liang, S., Sheng, H., Liu, Y., Hio, Z., Lu, Y. & Shen, H., *ZnO Schottky Ultraviolet Photodetectors*, J Cryst Growth, **225**, pp. 110-113, 2001.

[6] Minami, T., Ida, S., Miyata, T. & Minamino, Y., *Transparent Conducting ZnO Thin Films Deposited by Vacuum Arc Plasma Evaporation,* Thin Solid Films, **445**, pp. 268-273, 2003.

[7] Lee, J.B., Kim, H.J., Kim, S.G., Hwang, C.S., Hong, S.H. & Shin, Y.H., *Deposition of ZnO Thin Film by Magnetron Sputtering for a Film Bulk Acoustic Resonator,* Thin Solid Films, **435**, pp. 179-185, 2003.

[8] Jones, A., Jones, T.A., Mann, B. & Firth, J.G., *The Effect of the Physical Form of the Oxide on the Conductivity Changes Produced by CH_4, CO and H_2O on ZnO*, Sensors and Actuators, **5**, pp. 75-88, 1984.

[9] Hsueh, T. J. & Hsu, C.L., *Fabrication of Gas Sensing Devices with ZnO Nanostructure by The Low-Temperature Oxidation of Zinc Particles,* Sensors and Actuators B, **131**, pp. 572-576, 2008.

[10] Xu, J., Pan, Q., Shun, Y. & Tian, Z., *Grain Size Control and Gas Sensing Properties of ZnO Gas Sensor,* Sensors and Actuators B, **66**, pp. 277-279, 2000.

[11] Sadek, A., Wlodarski, W., Li, Y., Yu, W., Yu, X., Kalantar-Zadeh, K. & Li, X., *A ZnO Nanorod Based Layered ZnO/64^o YX $LiNbO_3$ SAW Hydrogen Gas Sensor,* Thin Solid Films, **515**, pp. 8705-8708, 2007.

[12] Yuliarto, B., Zhou, H.S., Yamada, T., Honma, I., Katsumura, Y. & Ichihara, M., *Preparation of Tin Modified Silica Mesoporous Films, Nanotechnology in Mesostructure Materials*, Studies in Surface Science and Catalysis, **146**, pp. 81-84, 2003.

[13] Yuliarto, B., Kumai, Y., Inagaki, S. & Zhou, H.S., *Enhanced Benzene Selectivity of Mesoporous Silica SPV Sensors by Incorporating Phenylene Groups in The Silica Framework,* Sensors and Actuators B: Chemical, **138**(2), pp. 417-21, 2009.

[14] Gao, T. & Wang, T.H., *Synthesis and Properties of Multipod-shaped ZnO Nanorods for Gas-Sensor Applications,* Appl. Phys. A, **80**, pp. 1451-1454, 2005.

[15] Tian, Z.R., Voigt, J.A., Liu, J., McKenzie, B., McDermott, M.J., Rodriguez, M.A., Konishi, H. & Xu, H., *Complex Oriented Semiconductor Nanostructures,* Nature Materials, **2**, pp. 821-826, 2003.

[16] Liu, F.T., Gao, S.F., Pei, S.K., Tseng, S.C. & Liu, C.H.J., *ZnO Nanorod Gas Sensor for NO_2 Detection,* Journal of the Taiwan Institute of Chemical Engineers, pp. 528-532, 2009.

[17] Hammer, M.S., Deibel, C., Rauh, D., Lorrmann, V. & Dyakonov, V., *Effect of Doping and Field-Induced Charge Carrier Density on The Electron Transport in Nanocrystalline ZnO,* Nanotechnology, **19**, pp. 48-57, 2008.

[18] Hsueh, T.J. & Hsu, C.L., *Fabrication of Gas Sensing Devices with ZnO Nanostructure by the Low-Temperature Oxidation of Zinc Particles,* Sensors and Actuators B, **131**, pp. 572-576, 2008.

[19] Guofeng, P., Ping, H., Ye, T. & Jingai, Q., *Gas Sensing Properties of Al-doped ZnO Thick Films Prepared by Sol-Gel Method*, ICMTMA, **2**, pp. 284-287, 2011.

[20] Trinh, T.T., Tu, N.H., Le, H.H, Ryu, K.Y., Le, K.B., Pillai, K. & Yi, J., *Improving the Ethanol Sensing of ZnO Nano-Particle Thin Film–the Correlation between the Grain Size and the Sensing Mechanism*, Sensors and Actuators B, **152**, pp. 73-81, 2011.

[21] United States Department of Labor, Occupational Safety and Health Administration, *Chemical Hazard and Toxic Substances*, retrieved from https://www.osha.gov/SLTC/hazardoustoxicsubstances/index.html, 2014.

[22] Lupan, O., Chai, G. & Chow, L., *Novel Hydrogen Gas Sensor based on single ZnO Nanorod*, Microelectronic Engineering, **85**(11), pp. 2220-2225, 2008.